 doi:10.20944/preprints202206.0057.v1

Article

Altered Rnome Expression in Murine Gastrocnemius Muscle Following Exposure to Jararhagin, a Metalloproteinase from Bothrops Jararaca Venom

Andrezza Nascimento[1], Bianca Cestari Zychar[2], Rodrigo Pessôa[1], Alberto José da Silva Duarte[3], Patricia Bianca Clissa[2,*,†] and Sabri Saeed Sanabani[3,4,*,†]

1 Post-graduation program in translational medicine, Federal University of São Paulo, São Paulo, Brazil; andrezza.ns@gmail.com, rodrigo_pessoa1@hotmail.com
2 Laboratory of Pathophysiology, Butantan Institute, São Paulo 05503-900, Brazil. bianca.zychar@butantan.gov.br
3 Laboratory of Dermatology and Immunodeficiency, Department of Dermatology LIM 56, Faculty of Medicine, University of São Paulo, São Paulo 05403 000, Brazil. alberto.duarte@hc.fm.usp.br
4 Laboratory of Immunopathology, Butantan Institute, São Paulo 05503-900, Brazil, patricia.clissa@butantan.gov.br
5 Laboratory of Medical Investigation Unit 03, Clinics Hospital, Faculty of Medicine, University of São Paulo, São Paulo 05403 000, Brazil. sabyem_63@yahoo.com
* Correspondence: SSS sabyem_63@yahoo.com ;.clissa@butantan.gov.br;
† These senior authors equally contributed

Abstract: Small RNAs (sRNA) and microRNAs (miRNAs) are small endogenous noncoding single-stranded RNAs that regulate gene expression in eukaryotes. Experiments in mice and humans have revealed that a typical small RNA can affect the expression of a wide range of genes, implying that small RNAs function as global regulators. Here, we used small RNA deep sequencing to investigate at how jararhagin, a metalloproteinase toxin produced from the venom of *Bothrops jararaca*, affected mmu-miRs expression in mice 2 h and 24 h after injection. The findings revealed that seven mmu-miRs were substantially differentially expressed (p-value (p (Corr) cut-off 0.05, FC 2) at 2h after jararhagin exposure, and that the majority of them were upregulated when compared to PBS. In contrast to these findings, a comparison of Jar 24h vs PBS 24hrs demonstrated that the majority of identified mmu-miRs were downregulated. Furthermore, the studies demonstrated that mmu-miR can target the expression of several genes involved in the MAPK signaling pathway. The steady antithetical regulation of mmu-miRs may correlates with the expression of genes that trigger apoptosis via MAPK in the early stages, and this effect intensifies with time. The findings expand our understanding of the effects of jararhagin on local tissue lesions at the molecular level.

Keywords: Small RNAs; Jararhagin; Venom

1. Introduction

Snakebite is a neglected disease in many tropical and subtropical developing countries. According to available data, the annual global death toll from snakebite envenoming is over 125,000, with an estimated 400,000 people suffering permanent physical disabilities and over 6 million disability-adjusted life years [1]. The majority of accidents reported to the Ministry of Health in Brazil are caused by venomous snakes of the Bothrops genus [2,3]. Bothropic envenomations are characterized by systemic reactions such as severe blood clotting disorders, as well as serious local reactions such as edema, pain, hemorrhage, and necrosis, and there may be large tissue losses with the possibility of amputations [4]. Clinically, serumtherapy is the only effective treatment for Bothrops envenoming; however, this approach is ineffective in reducing the fast setting local effects induced by the envenomation, implying that activation of endogenous mediators plays an important role in the local reaction [5]. Previous studies conducted by our group has shown

 doi:10.20944/preprints202206.0057.v1

that the pro-inflammatory effect of *Bothrops jararaca* venom is caused by the presence of metalloproteases in the venom [6,7]

The venom of *B. jararaca* is extremely protein-rich and contains a range of enzymes, including metalloproteases, serine proteinases, phospholipases (PLA2), and L-amino acid oxidases [8,9]. Several metalloproteases have been identified from the venom of *B. jararaca*, including bothropasin, HF3 [10] jararafibrase I [11], and jararhagin [12]. The best-characterized of these is the snake venom metalloproteinase jararhagin (SVMJ), which has a structure that includes the metalloproteinase domains, ECD-disintegrin domain (ECD: Glu-Cys-Asp), and cysteine-rich domain [5,12] characteristic of a PIII-type of snake venom metalloproteinase (SVMP)[13]. When jararhagin (Jar) is injected intradermal into mouse skin, hemorrhage occurs within minutes. This happens when basement membrane (BM) proteins like laminin, nidogen, and type IV collagen that surround endothelial cells in capillaries break down. This, along with the action of hemodynamic biophysical forces, can cause a mechanical disruption of BM structure, leading to local bleeding and, in some cases, a systemic effect (bleeding)[2,14]. The pro-inflammatory *in vivo* response induced by jararhagin is characterized by an increase in the adhesion and migration of leukocytes [15] with polymorphonucelar and mononuclear cells infiltrate [16] pro-inflammatory cytokines, TNF-α, IL-6 and IL-1β released in the local tissue damaged (LTD)[17] followed by mechanical hyperalgesia with the involvement of pro-inflammatory cytokines TNF-α and IL-1β, and nuclear transcription factor NFkB [18]. The chronic administration of jararhagin in the *in vivo* mouse sponge model demonstrate that this SVMP can modulate inflammatory angiogenesis, increasing inflammatory markers, as chemokines CXCL-1 and CCL2 and cytokine TNF-α, promoting neutrophil, and macrophage activation. Jararhagin also modulated the neovascularization increasing the VEGF levels, as well as fibrogenesis markers as TGF-β[19].

Small RNAs (sRNAs), which include MicroRNAs (miRNAs), are short endogenous, noncoding RNAs of 18–22 nucleotides in length that regulate gene expression at the post-transcriptional level by inhibiting translation or catalyzing gene degradation when bound to them via protein-mediated base-pairing[20]. These molecules play important roles in a variety of cellular processes, such as cell proliferation [21], differentiation [22], apoptosis [23], and inflammation [24]. The strict control of these miRNAs' expression is critical for controlling the progression of several diseases, including cancers [25] neurological diseases [26,27] and inflammatory disorders [28,29]. As a result, we hypothesized that miRNAs might play an important role in the events involved in the pathogenesis of the JARARHAGIN-induced tissue injury.

The goal of this study was to search for changes in sRNA levels in murine gastrocnemius muscle (MGM) two and twenty-four hours after intramuscular (i.m) jararhagin injection. We also investigated whether miRNA signatures identify some common mechanisms of tissue damage using target genes and pathway analysis.

2. Results

2.1. Known sRNA expression profile following jararhagin and PBS challenge

Here, we aimed to determine the role of sRNAs in jararhagin and PBS -induced innate immune response by measuring known sRNAs, novel sRNAs and mature miRNA levels in the gastrocnemius muscle at two-time points over 24 hours. To this end, the time-dependent changes in the sRNAs expression profile in RNA purified from gastrocnemius muscle at 2 h and 24 h were measured using Illumina MiSeq massive parallel sequencing (MPS) approach. Exposure to jararhagin resulted in a general dysregulation of 302 known sRNAs levels at both time points when compared to PBS (Table S1). Of the 302 known sRNA after 2 h of Jararahgin challenge, 19 were miRNA (13 downregulated and 6 upregulated), 124 snoRNA (77 downregulated and 47 upregulated), 33 snRNA (13 downregulated and 20 upregulated), and 126 tRNA (46 downregulated and 80 upregulated). The top ten significantly downregulated known sRNA were all snoRNAs (Snord68, Snord91,

Preprints (www.preprints.org) | NOT PEER-REVIEWED | Posted: 6 June 2022 doi:10.20944/preprints202206.0057.v1

Snora21, AF357341, Snord83, Snora69, Snora38, Snord88, Snord71)(average FC ≤ -25), whereas among the top ten significantly upregulated known sRNA (average FC > 25), five were tRNAs (trna107, trna994, trna699, trna110, and trna1747), four snoRNAs (U3 GENE ID : ENSMUSG00000094705, ENSMUSG00000093842, ENSMUSG00000094480, and ENSMUSG00000096428), one miRNA (mmu-mir-451a). Differential patterns of expression of the 302 known sRNAs at 24 h after challenge with jararhagin and PBS revealed five downregulated and 14 upregulated miRNAs, 23 downregulated and 101 upregulated snoRNAs, 6 downregulated and 27 upregulated snRNAs, and 27 downregulated and 99 upregulated tRNAs. Of these, the top ten significantly downregulated known sRNA were five snoRNAs (U3, SNORA8, SNORA66, SNORD13, and SNORA65), three tRNAs (trna91, trna979, and trna969), and two miRNAs (mmu-mir-6240 and mmu-mir-10a) (average FC ≤ -25), whereas the top ten considerably upregulated known sRNA were seven snoRNAs (SNORD20, SNORD44, AF357341, SNOU105B, SNORD8, SNORA57, and SNORA73a), one tRNAs (trna1432), and two miRNAs (mmu-mir-3535, mmu-mir-434) (average FC > 54). As shown in **figure 1**, there were 3 commonly dysregulated known sRNAs between entity list 1 (upregulated sRNAs in Jar 24hrs vs PBS24hrs) and entity list 4 (downregulated sRNAs in Jar 2hrs vs PBS2hrs), 14 sRNAs that were upregulated in entity list 1 (Jar 24hrs vs PBS24hrs) compared to entity list 3 (Jar 2hrs vs PBS2hrs), one downregulated sRNA between entity list 2 (Jar 24hrs vs PBS24hrs) and entity list 4 (Jar 2hrs vs PBS2hrs).

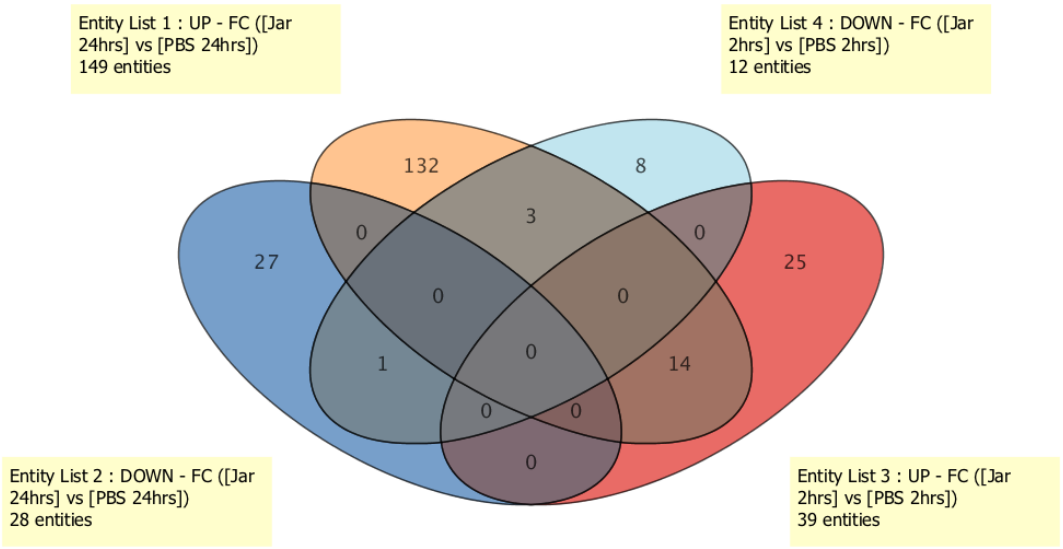

Figure 1. Venn diagram of known sRNA expression among groups

Preprints (www.preprints.org) | NOT PEER-REVIEWED | Posted: 6 June 2022 doi:10.20944/preprints202206.0057.v1

The expression analysis was repeated with a stringent statistical parameter of FDR p-value of < 0.05 and fold change of ≥ 5 and revealed 22 significantly dysregulated sRNAs. A heat map of the hierarchical clustering of the these sRNAs is shown in **Figure 2**.

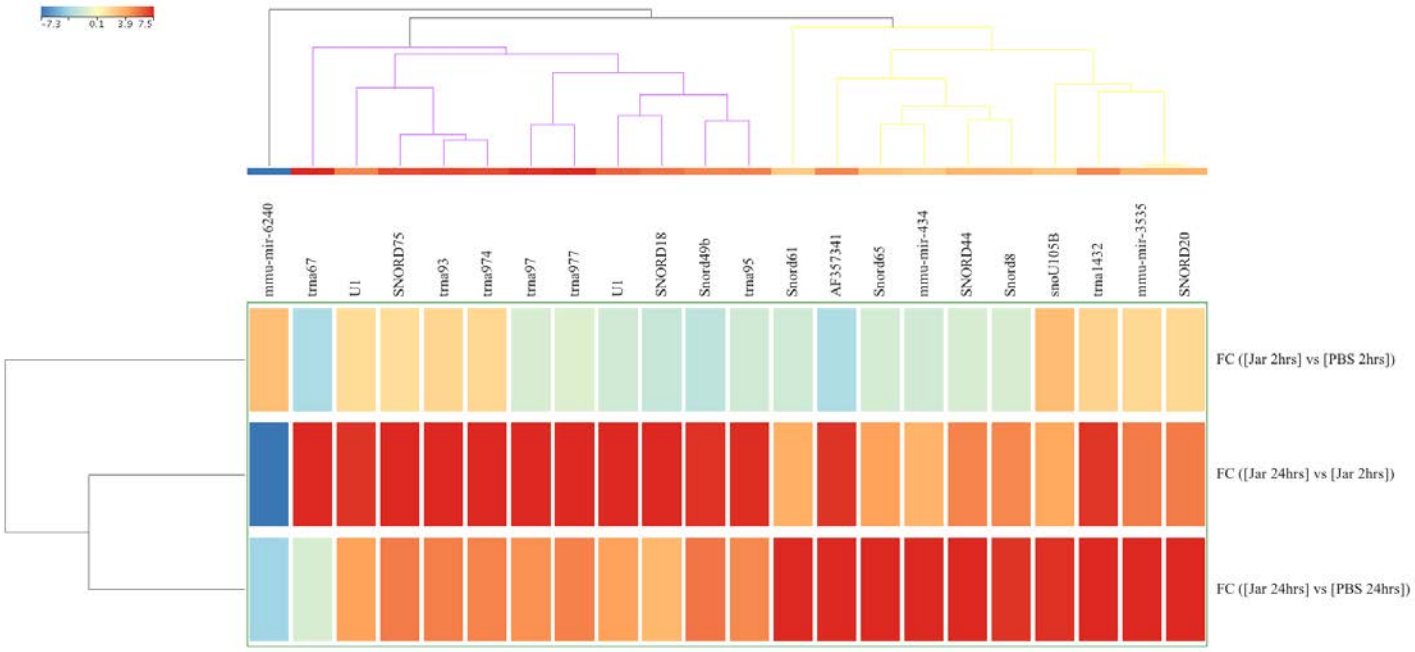

Figure 2. Differences in known small RNA (sRNA, n= 22) expression levels from gastrocnemius muscle samples obtained after 2 and 24 h of challenge with jararhagin and PBS. The sample-clustering tree is displayed to the left and the sRNA clustering tree is above. The color scale at the top indicates the relative expression levels of sRNA across all samples. Red indicates that the expression levels are higher compared with the mean, whereas blue indicates that the expression levels are lower compared with the mean. Each column represents one known sRNA and each row represents one sample.

Principal component analysis (PCA) was performed using the 22 strongly dysregulated sRNAs to visualize how closely related the four groups were regarding their sRNAs expression patterns (**Figure 3**). The results showed Jar 24 h and Jar 24 h as clearly separated clusters, while Jar 2h samples minimally overlapped with the PBS group. Overall, the results showed that the response was time-dependent and that sRNAs peaked at 24 h.

Preprints (www.preprints.org) | NOT PEER-REVIEWED | Posted: 6 June 2022 doi:10.20944/preprints202206.0057.v1

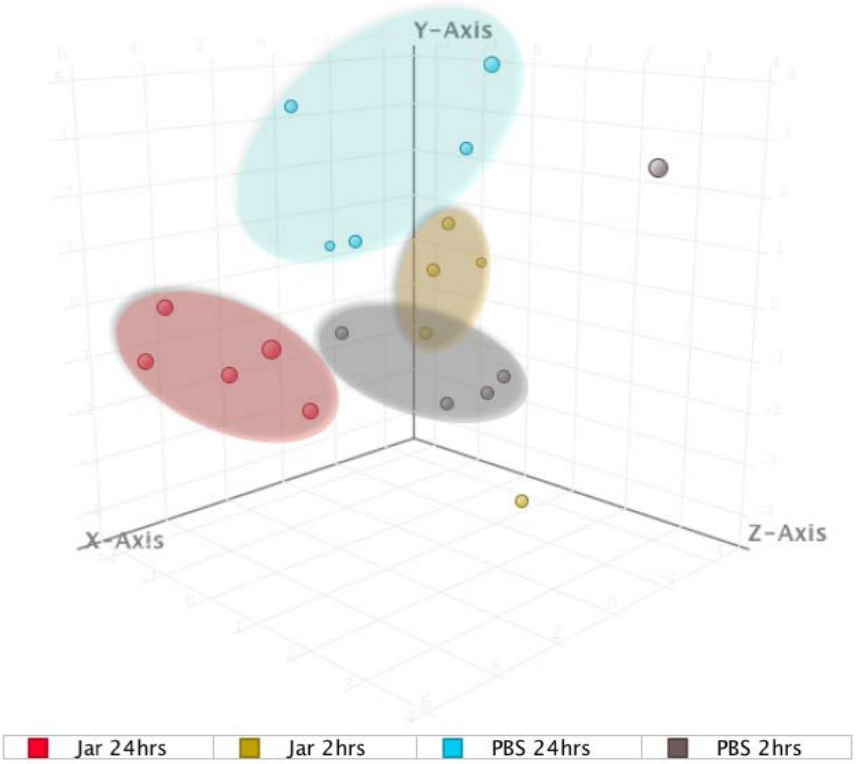

Figure 3. Principal Component Analysis (PCA) plot showing distances among the four groups based on the profile of the 22 significantly expressed known smallRNAs.

2.2. Novel sRNA expression profile following jararhagin and PBS challenge

A total of 3067 novel sRNAs were detected in all samples. Of these, 1851 (60.4%) were snoRNAs and 1216 (39.6%) were unknown novel sRNAs. Only 17 novel genes reached FDR significant value (p (Corr) cut-off < 0.05) and FC of ≥ 10 during the comparison of the JAR and PBS groups at two-time points. A comparison of the expression level of these genes between Jar 2h vs PBS 2hrs showed two unknown downregulated and 15 upregulated genes (8 snoRNAs and 7 unknown RNAs). The most significantly up and downregulated genes in this group were unknown sRNA (designated as NEWGENE1132, FC < -31.4 and NEWGENE25, FC > 13.4) (Table S2). Analysis of Jar 24h vs PBS 24hrs demonstrated 13 downregulated genes, of which eight were snoRNAs and five were unknown identities. Within this group, the snoRNA (NEWGENE1303) and unknown sRNA (NEWGENE1303) were the most significantly down (FC > -13) and upregulated (FC < 59.9) genes, respectively. The comparison between Jar 24h and Jar 2h revealed 14 downregulated genes and that half of them were snoRNAs. The top downregulated gene was snoRNA (NEWGENE2334, FC < -17.7). Three unknown genes within this group were upregulated, among which the gene designated as NEWGENE133 was the most upregulated novel gene in Jar 24hr compared to Jar 2 h (**Figure 4**).

Preprints (www.preprints.org) | NOT PEER-REVIEWED | Posted: 6 June 2022 doi:10.20944/preprints202206.0057.v1

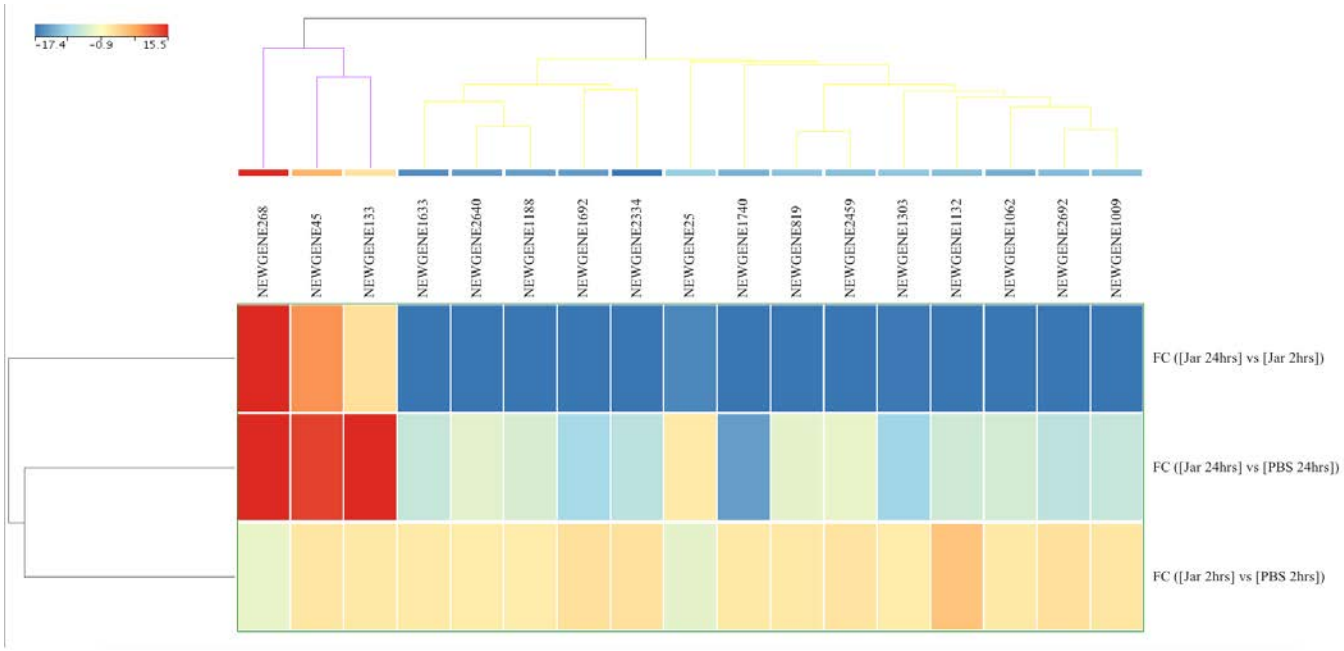

Figure 4. Differences in novel small RNA (sRNA, n= 17) expression levels from gastrocnemius muscle samples obtained after 2 and 24 h of challenge with jararhagin and PBS. The sample-clustering tree is displayed to the left and the sRNA clustering tree is above. The color scale at the top indicates the relative expression levels of sRNA across all samples. Red indicates that the expression levels are higher compared with the mean, whereas blue indicates that the expression levels are lower compared with the mean. Each column represents one known sRNA and each row represents one sample.

2.3. Mature miRNAs expression profile following jararhagin and PBS challenge

Investigation of mature mmu-miRNA among the jararhagin and PBS challenged groups at the two-time points revealed seven significantly dysregulated (*p*-value (p (Corr) cut-off < 0.05, FC ≥ 2) mmu-miRNAs (Table S3). Most of these mmu-miRS were significantly upregulated in Jar 2hrs vs PBS 2hrs. mmu-miR-486-5p was the most upregulated gene (FC > 22.7) followed by mmu-let-7f-5p (FC > 22). Opposite to the results of Jar 2hrs vs PBS 2hrs, the analysis of Jar 24h vs PBS 24hrs revealed that the majority of detected mmu-miRs were downregulated. mmu-miR-22-3p and -127-3p were the highest downregulated miRNAs (FC < -20). Of note, mmu-miR-22-3p was upregulated at 2hrs and downregulated at 24 h after challenge with jararhagin. Also, mmu-miR-22-3p expression was downregulated in a time-dependent manner ranging from FC < – 13 at 2hrs to FC -24.4 at 24 h compared to the PBS control group. The unsupervised hierarchical cluster analysis of the seven differentially expressed mature mmu-miRNAs of the three groups are displayed in **Figure 5**. In the PCA plot using the seven dysregulated mmu-miRs, the Jar 2hrs and Jar 24hrs samples clustered into two distinct groups (**Figure 6**). Furthermore, the Jar 24hrs samples showed a higher degree of heterogeneity and minimal overlap with both the Jar 2hrs, PBS 2hrs, and/or 24hrs samples. Overall, the PCA plot showed that mmu-miRNAs can separate gastrocnemius muscle challenged with jararhagin at 24 h from samples challenged at 2hrs as well as PBS 2hrs from PBS 2hrs.

2.4. Target genes, KEGG pathway, and GO enrichment analysis

To investigate the possible functions of the seven mmu-miRNAs in immune response towards the JARARHAGIN, MirWalk v3 online tool was used to predict target genes and pathways potentially influenced by these mmu-miRNAs. In total, 175 unique genes were predicted by at least three prediction tools for four miRNAs, namely mmu-miR-22-3p, 127-3p, 143-3p, and mmu-let-7f-5p (Table S4). mmu-miR-22-3p exhibited 56 target genes whereas mmu-miR-127-3p exhibited three target genes (Slc12a4, Spock2, Septin7), mmu-miR-143-3p 33 target genes, and mmu-let-7f-5p 83 target genes. There were eight KEGG

Preprints (www.preprints.org) | NOT PEER-REVIEWED | Posted: 6 June 2022 doi:10.20944/preprints202206.0057.v1

pathways enriched with genes targeted by the four miRNAs, among which the most statistically significant pathway was the MAPK_signaling_pathway (mmu04010, FDR corrected *p*-value = 0.0038) (Table S5). Subsequently, GO annotations were performed by the predicted target genes (Table S5). The GOBP enrichment results showed that norepinephrine-epinephrine-mediated vasodilation involved in regulation of systemic arterial blood pressure (GO:0002025) and activin receptor signaling pathway (GO:0032924) were the top significantly enriched processes (FDR corrected *p*-value of ≤0.05). In the CC category, the target genes were significantly enriched in the various processes including chromatin (GO:0000785), T-tubule (GO:0030315), nuclear envelope (GO:0005635), and Schaffer collateral - CA1 synapse (GO:0098685). In the MF category, the target genes were significantly and mainly enriched in guanyl-nucleotide exchange factor activity (GO:0005085) and DNA-binding transcription factor activity (GO:0003700).

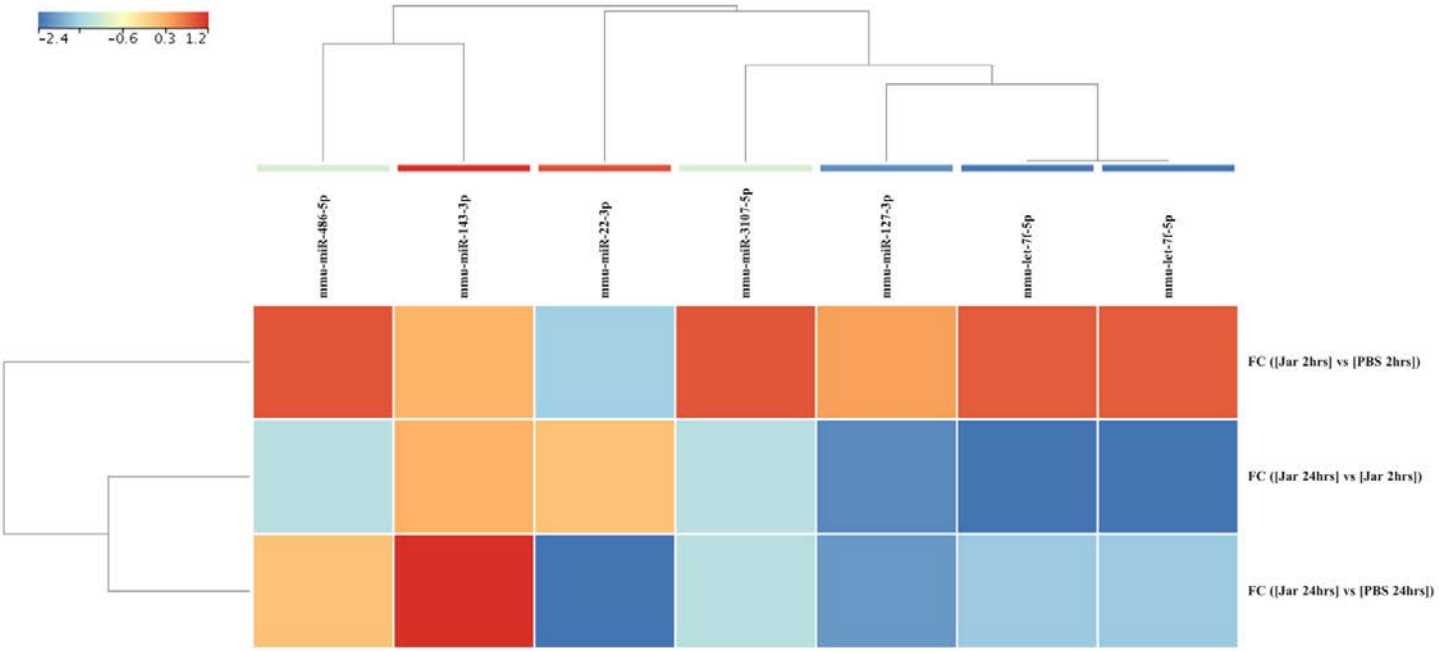

Figure 5. Differences in mature mmu-miRNA (n= 7) expression levels from gastrocnemius muscle samples obtained after 2 and 24 h of challenge with jararhagin and PBS. The sample-clustering tree is displayed to the left and the sRNA clustering tree is above. The color scale at the top indicates the relative expression levels of sRNA across all samples. Red indicates that the expression levels are higher compared with the mean, whereas blue indicates that the expression levels are lower compared with the mean. Each column represents one known sRNA and each row represents one sample..

 doi:10.20944/preprints202206.0057.v1

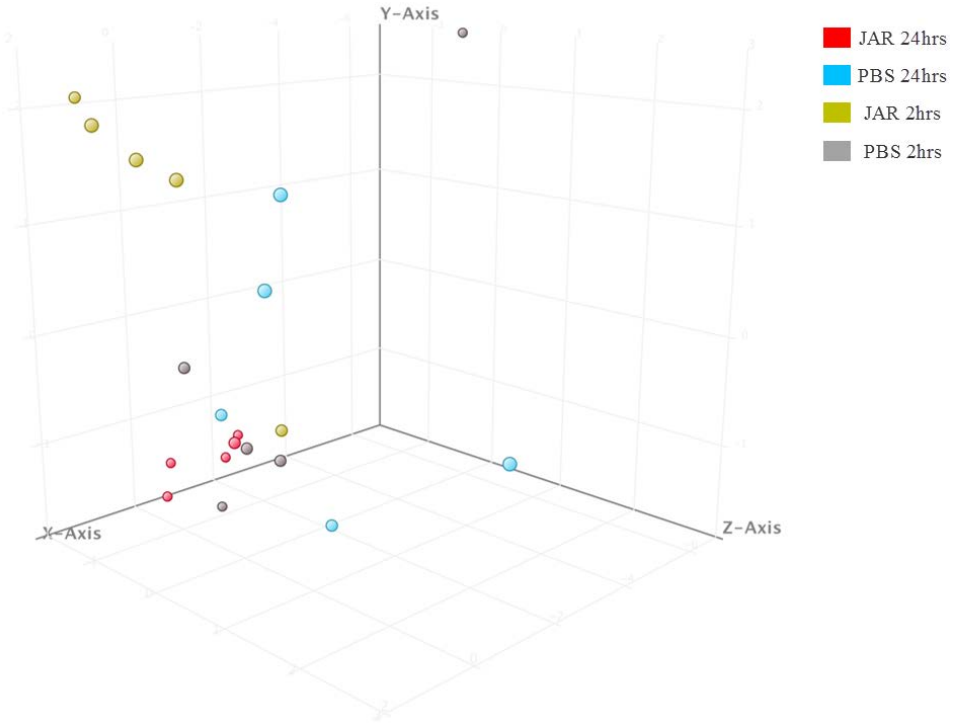

Figure 6. Principal Component Analysis (PCA) plot showing distances among the four groups based on the profile of the seven significantly expressed mmu-miRNAs.

3. Discussion

The JARARHAGIN triggers activation of innate immune cells and causes strong pro-inflammatory response characterized by marked recruitment and accumulation of leukocyte at the inflammation site, induction of pro-inflammatory cytokines and apoptotic macrophages [16,17,30,31]. It is believed that alterations in molecular processes are at least partially mediate these events [32,33]. Several studies have demonstrated snake venom to exhibit geographic and ontogenetic variation [33-35]. To date, no reports are available on the sRNA sequencing profiling of the injured tissue as a result of snake bite. Nevertheless, numerous studies have demonstrated the roles of miRNAs in many biological events, including cell death, differentiation, proliferation, and cell growth [36,37]. Here, we generated wide genome small RNA sequencing data from mice gastrocnemius muscle challenged with the JARARHAGIN at two-time points to investigate the temporal role of sRNAome in the JARARHAGIN–injured tissue. Our study reveals that the expression levels of miRNAs alter when local tissues are exposed to jararhagin, indicating a role for miRNAs in the cellular response to the SVMP in these tissues. This may indicate that local tissues employ the activation and transcription of miRNAs, as well as gene translation, two hours after exposure. It is also possible that the synthesis of miRNAs begins early on in the inflammatory response of these local lesions to jararhagin. Furthermore, we show that miRNA temporal expression alterations in response to jararhagin are different in local lesions. Two hours after challenge, we identified the dysregulation of 302 sRNAs. Among them, 18 sRNA transcripts were dysregulated at 24 h after challenge (Figure 1). Our results also demonstrate that mum-miRNAs, particularly mmu-miR-22-3p, 127-3p, 143-3p, and mmu-let-7f-5p are actively dysregulated at both time points. We also found that the four altered mmu-miR converge on the MAPK_signaling_pathway. Of note, the MAPK signaling pathway has been shown to mediate the activation of intracellular PLA2s in physiologic and inflammatory contexts [38,39]. Thus, we assume that implication of MAPK signaling pathway as an underlying pathogenic mechanism in the JARARHAGIN–injured tissue.

 doi:10.20944/preprints202206.0057.v1

Here, we show that the tissue levels of mum-miRNA-22-3p in mice challenged with jararhagin are considerably lowered at 2 hours and continue to decline at 24 hours. Although a link between mum-miRNA-22-3p and tissue damage caused by the B. jararaca venom has not been previously reported, miR-22-3p in human has been linked to other chronic inflammatory diseases. For example, miR-22-3p has been reported to be elevated in B cells from systemic lupus erythematosus subjects compared to healthy human subjects [40]. Additionally, Pei et al. [41] recently reported that miR-22-3p levels are elevated in peripheral CD4+ T cells in inflammatory bowel disease. Inhibition of miR-22 was linked to increased astrogliosis [42], and its overexpression has been shown to protect against brain injury in animal models [43]. In the study by Jovicic et al. [43], miR-22 was also shown to reduce apoptosis, as evidenced by its ability to inhibit effector caspase activation in Huntington's disease. So far, no study has evaluated the role of miRNA-22-3p in the affected tissue following B. jararaca bite. It is tempting to speculate that the effect of the sever tissue injury is mediated, at least in part, by its targeting pro-apoptotic genes MAPK. Targeting of broad anti-apoptotic and MAPK pathways, as well as evidence that it is downregulated in injured tissue, make miR-22 an especially intriguing approach for treating tissue damage and inflammation following B. jararaca bite.

Regarding the mmu-miR-127-3p, it was recently demonstrated that this miR in mouse skin wounds triggered a prolonged cell cycle arrest with unique molecular hallmarks of senescence, including activation of the senescence-associated -galactosidase, increase in p53 and p21 levels, inhibition of lamin B1, proliferation factors, and the production of senescence-associated inflammatory and extracellular matrixremodeling components. [44]. Several studies demonstrated miR-127-3p plays a major anti-tumor role in various cancers [45-47]. The results recently reported by DU et al [48] revealed that the MAPK4 gene was a new candidate gene and might be a target gene for miR-127-3p in ovarian cancer. In our study we showed that mmu-miR-127-3p was downregulated after challenge with jararhagin at both time points. Although speculative, a possible scenario is that the downregulation of mmu-miR-127-3p resulted in upregulation of MAPK pathways as MAPK is a direct target for mmu-miR-127.

Although we evaluated the expression of sRNA, including mature mm-miRNA, in local lesions, a prospective validation study is required to establish their levels or expression of their predicted target genes. Another limitation is that we restricted our study and interpretation mostly to miRNA.

4. Materials and Methods

4.1. Samples

Male Swiss mice weighing 20–25 g were obtained from the Instituto Butantan's housing facility. Before the experiments, the animals were kept 48 h in a 12:12 h light:dark cycle and had access to food and water ad libitum. All experimental procedures were carried out in accordance with the ethical standards proposed by the International Society of Toxinology and the Brazilian College of Experimental Animals, and were approved by the Butantan Institute's Ethical Committee for the Use of Animals (CEAU n 2614060420). To determine the inflammatory response induced by JARARHAGIN, ten mice were separated into two groups of five. Both groups were challenged with 1 µg of JARARHAGIN i.m. into the gastrocnemius muscle in the right paw and phosphate-buffered saline (PBS) in the left paw. Mice were scarified after 2 h and 24 h, and muscles from the right paw (designated Jar 2 and 24hrs) and left paw (designated PBS 2 and 24hrs) were dissected, minced, and cells were harvested in TRIzol and stored at -80 °C until use.

4.2. RNA extraction

Each gastrocnemius muscle sample was separately homogenized and RNA was extracted using the miRCURY RNA Isolation kit (Exqon,Vedbæk, Denmark) according to the manufacturer's instructions. The resulting RNA was eluted with RNase-free water and

 doi:10.20944/preprints202206.0057.v1

stored at −80 °C until further use. sRNAs quantities were measured using a Qubit 2.0 fluorometer with microRNA Assay Kit, respectively (Thermo Fisher Scientific, Inc.).

4.3. Library construction

For each sample in both groups, sRNA libraries were prepared with the TruSeq Small RNA sample preparation kit (Illumina, San Diego, CA) per the manufacturer's instructions and a previously published protocol [49,50]. A total library pool of 4 nM was prepared using a MiSeq Reagent Kit v3 150 cycle followed by sequencing on a MiSeq system (Illumina, San Diego, CA, USA). The libraries were sequenced on a 150-SE run on the MiSeq with a 36-base single-end protocol [51]. After trimming adapter sequences and sequence quality testing, each library's raw data were aligned to the human reference genome (hg19), then combined to an expression matrix and processed with the Strand NGS version 3.1 (Strand Life Science). The distributions of the sRNA data in each clinical condition were conducted according to the quantile normalization algorithm, with a baseline transformation set to the median of all samples. Only miRNAs with more than ten copies were considered for subsequent analysis. miRNAs with a fold-change ≥2 were supposed to be differentially expressed. All sequence data described here are available in the online Zenodo repository : https://doi.org/10.5281/zenodo.6599508

4.4. Functional annotation and pathway analysis of miRNA target genes

The target genes from differentially expressed miRNAs of HAM and ASP versus HC groups were predicted by miRWalk 3.0 algorithm. After obtaining a list of putative and experimentally validated targets relative to each miRNA, we further scanned these targets and analyzed them for Gene Ontology (GO) enrichment terms and Kyoto Encyclopedia of Genes and Genomes (KEGG) pathway classification. The target genes for the significantly dysregulated miRNA were interrogated for significant well-curated signaling pathways obtained from Reactome using MirWalk v.3 (Mar/2020 update) sorted by p-value ranking <0.05 using Benjamini-Hochberg multiple testing correction to control the false discovery rate (FDR).

4.5. Constructing regulatory network between miRNAs and their targets

The posttranscriptional gene regulatory network is defined as a directed and bipartite network in which expressions of miRNA-target gene interacting pairs are reversely correlated. The analysis of the network for the interaction of miRNA-messenger RNA (mRNA) putative target was performed using the miRWalk network algorithm [52].

5. Conclusions

In conclusion, our study provides additional evidence that jararhagin promotes a time-dependent change in the expression levels of miRNAs, suggesting their role in the cellular response to tissue injury. In addition, we show evidence that, in response to venom exposure, distinct miRNAs are downregulated at distinct time points in local lesions. Studies addressing the mechanisms underlying the steady reduction of the miRNA described in this study are warranted. Understanding of the involvement of microRNAs in tissue injury caused by SVMP jararhagin and identification of their specific targets in local lesions warrants additional investigation that may lead to the development of novel therapeutic approaches for tissue injury.

Supplementary Materials: The following supporting information can be downloaded at: www.mdpi.com/xxx/s1, Figure S1: title; Table S1: title; Video S1: title.

Conflicts of Interest: The authors declare no conflict of interest.

References

1. Knudsen, C.; Jürgensen, J.A.; Føns, S.; Haack, A.M.; Friis, R.U.W.; Dam, S.H.; Bush, S.P.; White, J.; Laustsen, A.H. Snakebite Envenoming Diagnosis and Diagnostics. *Frontiers in Immunology* **2021**, *12*, doi:10.3389/fimmu.2021.661457.
2. Baldo, C.; Jamora, C.; Yamanouye, N.; Zorn, T.M.; Moura-da-Silva, A.M. Mechanisms of vascular damage by hemorrhagic snake venom metalloproteinases: tissue distribution and in situ hydrolysis. *PLoS Negl Trop Dis* **2010**, *4*, e727, doi:10.1371/journal.pntd.0000727.
3. Ministério-da-Saúde. Acidente por animais peçonhentos - Descrição da doença. Available online: Available from: https://www.saude.gov.br/saude-de-a-z/acidentes-por-animais-peconhentos/13713-descricao-da-doenca (accessed on 28/03/20).
4. Cardoso, J.L.; Fan, H.W.; Franca, F.O.; Jorge, M.T.; Leite, R.P.; Nishioka, S.A.; Avila, A.; Sano-Martins, I.S.; Tomy, S.C.; Santoro, M.L.; et al. Randomized comparative trial of three antivenoms in the treatment of envenoming by lance-headed vipers (Bothrops jararaca) in Sao Paulo, Brazil. *The Quarterly journal of medicine* **1993**, *86*, 315-325.
5. Moura-da-Silva, A.M.; Baldo, C. Jararhagin, a hemorrhagic snake venom metalloproteinase from Bothrops jararaca. *Toxicon* **2012**, *60*, 280-289, doi:10.1016/j.toxicon.2012.03.026.
6. Araujo, S.D.; de Souza, A.; Nunes, F.P.; Goncalves, L.R. Effect of dexamethasone associated with serum therapy on treatment of Bothrops jararaca venom-induced paw edema in mice. *Inflammation research : official journal of the European Histamine Research Society ... [et al.]* **2007**, *56*, 409-413, doi:10.1007/s00011-007-7054-x.
7. Zychar, B.C.; Dale, C.S.; Demarchi, D.S.; Goncalves, L.R. Contribution of metalloproteases, serine proteases and phospholipases A2 to the inflammatory reaction induced by Bothrops jararaca crude venom in mice. *Toxicon* **2010**, *55*, 227-234, doi:10.1016/j.toxicon.2009.07.025.
8. Cidade, D.A.; Simao, T.A.; Davila, A.M.; Wagner, G.; Junqueira-de-Azevedo, I.L.; Ho, P.L.; Bon, C.; Zingali, R.B.; Albano, R.M. Bothrops jararaca venom gland transcriptome: analysis of the gene expression pattern. *Toxicon* **2006**, *48*, 437-461, doi:10.1016/j.toxicon.2006.07.008.
9. Pereira, L.M.; Messias, E.A.; Sorroche, B.P.; Oliveira, A.D.N.; Arantes, L.; de Carvalho, A.C.; Tanaka-Azevedo, A.M.; Grego, K.F.; Carvalho, A.L.; Melendez, M.E. In-depth transcriptome reveals the potential biotechnological application of Bothrops jararaca venom gland. *The journal of venomous animals and toxins including tropical diseases* **2020**, *26*, e20190058, doi:10.1590/1678-9199-JVATITD-2019-0058.
10. Assakura, M.T.; Reichl, A.P.; Mandelbaum, F.R. Comparison of immunological, biochemical and biophysical properties of three hemorrhagic factors isolated from the venom of Bothrops jararaca (jararaca). *Toxicon* **1986**, *24*, 943-946, doi:10.1016/0041-0101(86)90094-2.
11. Maruyama, M.; Sugiki, M.; Yoshida, E.; Mihara, H.; Nakajima, N. Purification and characterization of two fibrinolytic enzymes from Bothrops jararaca (jararaca) venom. *Toxicon* **1992**, *30*, 853-864, doi:10.1016/0041-0101(92)90383-g.
12. Paine, M.J.; Desmond, H.P.; Theakston, R.D.; Crampton, J.M. Purification, cloning, and molecular characterization of a high molecular weight hemorrhagic metalloprotease, jararhagin, from Bothrops jararaca venom. Insights into the disintegrin gene family. *The Journal of biological chemistry* **1992**, *267*, 22869-22876.
13. Fox, J.W.; Serrano, S.M. Insights into and speculations about snake venom metalloproteinase (SVMP) synthesis, folding and disulfide bond formation and their contribution to venom complexity. *The FEBS journal* **2008**, *275*, 3016-3030, doi:10.1111/j.1742-4658.2008.06466.x.
14. Escalante, T.; Shannon, J.; Moura-da-Silva, A.M.; Gutierrez, J.M.; Fox, J.W. Novel insights into capillary vessel basement membrane damage by snake venom hemorrhagic metalloproteinases: a biochemical and

immunohistochemical study. *Archives of biochemistry and biophysics* **2006**, *455*, 144-153, doi:10.1016/j.abb.2006.09.018.

15. Zychar, B.C.; Clissa, P.B.; Carvalho, E.; Alves, A.S.; Baldo, C.; Faquim-Mauro, E.L.; Goncalves, L.R.C. Modulation of Adhesion Molecules Expression by Different Metalloproteases Isolated from Bothrops Snakes. *Toxins* **2021**, *13*, doi:10.3390/toxins13110803.
16. Costa, E.P.; Clissa, P.B.; Teixeira, C.F.; Moura-da-Silva, A.M. Importance of metalloproteinases and macrophages in viper snake envenomation-induced local inflammation. *Inflammation* **2002**, *26*, 13-17, doi:10.1023/a:1014465611487.
17. Clissa, P.B.; Lopes-Ferreira, M.; Della-Casa, M.S.; Farsky, S.H.; Moura-da-Silva, A.M. Importance of jararhagin disintegrin-like and cysteine-rich domains in the early events of local inflammatory response. *Toxicon* **2006**, *47*, 591-596, doi:10.1016/j.toxicon.2006.02.001.
18. Ferraz, C.R.; Calixto-Campos, C.; Manchope, M.F.; Casagrande, R.; Clissa, P.B.; Baldo, C.; Verri, W.A., Jr. Jararhagin-induced mechanical hyperalgesia depends on TNF-alpha, IL-1beta and NFkappaB in mice. *Toxicon* **2015**, *103*, 119-128, doi:10.1016/j.toxicon.2015.06.024.
19. Ferreira, B.A.; Deconte, S.R.; de Moura, F.B.R.; Tomiosso, T.C.; Clissa, P.B.; Andrade, S.P.; Araujo, F.A. Inflammation, angiogenesis and fibrogenesis are differentially modulated by distinct domains of the snake venom metalloproteinase jararhagin. *International journal of biological macromolecules* **2018**, *119*, 1179-1187, doi:10.1016/j.ijbiomac.2018.08.051.
20. Valencia-Sanchez, M.A.; Liu, J.; Hannon, G.J.; Parker, R. Control of translation and mRNA degradation by miRNAs and siRNAs. *Genes & development* **2006**, *20*, 515-524, doi:10.1101/gad.1399806.
21. Brennecke, J.; Hipfner, D.R.; Stark, A.; Russell, R.B.; Cohen, S.M. bantam encodes a developmentally regulated microRNA that controls cell proliferation and regulates the proapoptotic gene hid in Drosophila. *Cell* **2003**, *113*, 25-36, doi:10.1016/s0092-8674(03)00231-9.
22. Wienholds, E.; Koudijs, M.J.; van Eeden, F.J.; Cuppen, E.; Plasterk, R.H. The microRNA-producing enzyme Dicer1 is essential for zebrafish development. *Nature genetics* **2003**, *35*, 217-218, doi:10.1038/ng1251.
23. Xu, P.; Vernooy, S.Y.; Guo, M.; Hay, B.A. The Drosophila microRNA Mir-14 suppresses cell death and is required for normal fat metabolism. *Current biology : CB* **2003**, *13*, 790-795, doi:10.1016/s0960-9822(03)00250-1.
24. Ardekani, A.M.; Naeini, M.M. The Role of MicroRNAs in Human Diseases. *Avicenna journal of medical biotechnology* **2010**, *2*, 161-179.
25. Naidu, S.; Magee, P.; Garofalo, M. MiRNA-based therapeutic intervention of cancer. *Journal of hematology & oncology* **2015**, *8*, 68, doi:10.1186/s13045-015-0162-0.
26. Rao, P.; Benito, E.; Fischer, A. MicroRNAs as biomarkers for CNS disease. *Frontiers in molecular neuroscience* **2013**, *6*, 39, doi:10.3389/fnmol.2013.00039.
27. Shafi, G.; Aliya, N.; Munshi, A. MicroRNA signatures in neurological disorders. *The Canadian journal of neurological sciences. Le journal canadien des sciences neurologiques* **2010**, *37*, 177-185, doi:10.1017/s0317167100009902.
28. Garo, L.P.; Ajay, A.K.; Fujiwara, M.; Gabriely, G.; Raheja, R.; Kuhn, C.; Kenyon, B.; Skillin, N.; Kadowaki-Saga, R.; Saxena, S.; et al. MicroRNA-146a limits tumorigenic inflammation in colorectal cancer. *Nature communications* **2021**, *12*, 2419, doi:10.1038/s41467-021-22641-y.
29. Liu, P.; Hu, L.; Shi, Y.; Liu, Y.; Yu, G.; Zhou, Y.; An, Q.; Zhu, W. Changes in the Small RNA Expression in Endothelial Cells in Response to Inflammatory Stimulation. *Oxidative medicine and cellular longevity* **2021**, *2021*, 8845520, doi:10.1155/2021/8845520.

30. Clissa, P.B.; Laing, G.D.; Theakston, R.D.; Mota, I.; Taylor, M.J.; Moura-da-Silva, A.M. The effect of jararhagin, a metalloproteinase from Bothrops jararaca venom, on pro-inflammatory cytokines released by murine peritoneal adherent cells. *Toxicon* **2001**, *39*, 1567-1573, doi:10.1016/s0041-0101(01)00131-3.
31. Gallagher, P.; Bao, Y.; Serrano, S.M.; Laing, G.D.; Theakston, R.D.; Gutierrez, J.M.; Escalante, T.; Zigrino, P.; Moura-da-Silva, A.M.; Nischt, R.; et al. Role of the snake venom toxin jararhagin in proinflammatory pathogenesis: in vitro and in vivo gene expression analysis of the effects of the toxin. *Archives of biochemistry and biophysics* **2005**, *441*, 1-15, doi:10.1016/j.abb.2005.06.007.
32. Vonk, F.J.; Casewell, N.R.; Henkel, C.V.; Heimberg, A.M.; Jansen, H.J.; McCleary, R.J.; Kerkkamp, H.M.; Vos, R.A.; Guerreiro, I.; Calvete, J.J.; et al. The king cobra genome reveals dynamic gene evolution and adaptation in the snake venom system. *Proc Natl Acad Sci U S A* **2013**, *110*, 20651-20656, doi:10.1073/pnas.1314702110.
33. Durban, J.; Perez, A.; Sanz, L.; Gomez, A.; Bonilla, F.; Rodriguez, S.; Chacon, D.; Sasa, M.; Angulo, Y.; Gutierrez, J.M.; et al. Integrated "omics" profiling indicates that miRNAs are modulators of the ontogenetic venom composition shift in the Central American rattlesnake, Crotalus simus simus. *BMC Genomics* **2013**, *14*, 234, doi:10.1186/1471-2164-14-234.
34. Guercio, R.A.; Shevchenko, A.; Shevchenko, A.; Lopez-Lozano, J.L.; Paba, J.; Sousa, M.V.; Ricart, C.A. Ontogenetic variations in the venom proteome of the Amazonian snake Bothrops atrox. *Proteome science* **2006**, *4*, 11, doi:10.1186/1477-5956-4-11.
35. Calvete, J.J.; Sanz, L.; Cid, P.; de la Torre, P.; Flores-Diaz, M.; Dos Santos, M.C.; Borges, A.; Bremo, A.; Angulo, Y.; Lomonte, B.; et al. Snake venomics of the Central American rattlesnake Crotalus simus and the South American Crotalus durissus complex points to neurotoxicity as an adaptive paedomorphic trend along Crotalus dispersal in South America. *Journal of proteome research* **2010**, *9*, 528-544, doi:10.1021/pr9008749.
36. He, L.; Hannon, G.J. MicroRNAs: small RNAs with a big role in gene regulation. *Nature reviews. Genetics* **2004**, *5*, 522-531, doi:10.1038/nrg1379.
37. O'Brien, J.; Hayder, H.; Zayed, Y.; Peng, C. Overview of MicroRNA Biogenesis, Mechanisms of Actions, and Circulation. *Frontiers in endocrinology* **2018**, *9*, 402, doi:10.3389/fendo.2018.00402.
38. Hu, S.B.; Zou, Q.; Lv, X.; Zhou, R.L.; Niu, X.; Weng, C.; Chen, F.; Fan, Y.W.; Deng, Z.Y.; Li, J. 9t18:1 and 11t18:1 activate the MAPK pathway to regulate the expression of PLA2 and cause inflammation in HUVECs. *Food & function* **2020**, *11*, 649-661, doi:10.1039/c9fo01982k.
39. Andersson, L.; Bostrom, P.; Ericson, J.; Rutberg, M.; Magnusson, B.; Marchesan, D.; Ruiz, M.; Asp, L.; Huang, P.; Frohman, M.A.; et al. PLD1 and ERK2 regulate cytosolic lipid droplet formation. *Journal of cell science* **2006**, *119*, 2246-2257, doi:10.1242/jcs.02941.
40. Wu, X.N.; Ye, Y.X.; Niu, J.W.; Li, Y.; Li, X.; You, X.; Chen, H.; Zhao, L.D.; Zeng, X.F.; Zhang, F.C.; et al. Defective PTEN regulation contributes to B cell hyperresponsiveness in systemic lupus erythematosus. *Science translational medicine* **2014**, *6*, 246ra299, doi:10.1126/scitranslmed.3009131.
41. Pei, X.F.; Cao, L.L.; Huang, F.; Qiao, X.; Yu, J.; Ye, H.; Xi, C.L.; Zhou, Q.C.; Zhang, G.F.; Gong, Z.L. Role of miR-22 in intestinal mucosa tissues and peripheral blood CD4+ T cells of inflammatory bowel disease. *Pathology, research and practice* **2018**, *214*, 1095-1104, doi:10.1016/j.prp.2018.04.009.
42. Jimenez-Mateos, E.M.; Arribas-Blazquez, M.; Sanz-Rodriguez, A.; Concannon, C.; Olivos-Ore, L.A.; Reschke, C.R.; Mooney, C.M.; Mooney, C.; Lugara, E.; Morgan, J.; et al. microRNA targeting of the P2X7 purinoceptor opposes a contralateral epileptogenic focus in the hippocampus. *Scientific reports* **2015**, *5*, 17486, doi:10.1038/srep17486.

43. Jovicic, A.; Zaldivar Jolissaint, J.F.; Moser, R.; Silva Santos Mde, F.; Luthi-Carter, R. MicroRNA-22 (miR-22) overexpression is neuroprotective via general anti-apoptotic effects and may also target specific Huntington's disease-related mechanisms. *PloS one* **2013**, *8*, e54222, doi:10.1371/journal.pone.0054222.
44. Auler, M.; Bergmeier, V.; Georgieva, V.S.; Pitzler, L.; Frie, C.; Nuchel, J.; Eckes, B.; Hinz, B.; Brachvogel, B. miR-127-3p Is an Epigenetic Activator of Myofibroblast Senescence Situated within the MicroRNA-Enriched Dlk1-Dio3Imprinted Domain on Mouse Chromosome 12. *The Journal of investigative dermatology* **2021**, *141*, 1076-1086 e1073, doi:10.1016/j.jid.2020.11.011.
45. Lu, M.; Ju, S.; Shen, X.; Wang, X.; Jing, R.; Yang, C.; Chu, H.; Cong, H. Combined detection of plasma miR-127-3p and HE4 improves the diagnostic efficacy of breast cancer. *Cancer biomarkers : section A of Disease markers* **2017**, *18*, 143-148, doi:10.3233/CBM-160024.
46. Guo, L.H.; Li, H.; Wang, F.; Yu, J.; He, J.S. The Tumor Suppressor Roles of miR-433 and miR-127 in Gastric Cancer. *International journal of molecular sciences* **2013**, *14*, 14171-14184, doi:10.3390/ijms140714171.
47. Calin, G.A.; Croce, C.M. MicroRNA signatures in human cancers. *Nature reviews. Cancer* **2006**, *6*, 857-866, doi:10.1038/nrc1997.
48. Du, S.Y.; Huang, X.X.; Li, N.M.; Lv, C.Y.; Lv, C.H.; Wei, M.L.; Gao, Z.; Zhang, Y.P. MiR-127-3p inhibits proliferation of ovarian cancer in rats through down-regulating MAPK4. *European review for medical and pharmacological sciences* **2020**, *24*, 10383-10390, doi:10.26355/eurrev_202010_23388.
49. Clissa, P.B.; Pessoa, R.; Ferraz, K.F.; de Souza, D.R.; Sanabani, S.S. Data on global expression of non-coding RNome in mice gastrocnemius muscle exposed to jararhagin, snake venom metalloproteinase. *Data in brief* **2016**, *9*, 685-688, doi:10.1016/j.dib.2016.09.052.
50. Valadao de Souza, D.R.; Pessoa, R.; Nascimento, A.; Nukui, Y.; Pereira, J.; Casseb, J.; Penalva de Oliveira, A.C.; da Silva Duarte, A.J.; Clissa, P.B.; Sanabani, S.S. Small RNA profiles of HTLV-1 asymptomatic carriers with monoclonal and polyclonal rearrangement of the T-cell antigen receptor gamma-chain using massively parallel sequencing: A pilot study. *Oncology letters* **2020**, *20*, 2311-2321, doi:10.3892/ol.2020.11803.
51. Nascimento, A.; Valadao de Souza, D.R.; Pessoa, R.; Pietrobon, A.J.; Nukui, Y.; Pereira, J.; Casseb, J.; Penalva de Oliveira, A.C.; Loureiro, P.; da Silva Duarte, A.J.; et al. Global expression of noncoding RNome reveals dysregulation of small RNAs in patients with HTLV-1-associated adult T-cell leukemia: a pilot study. *Infectious agents and cancer* **2021**, *16*, 4, doi:10.1186/s13027-020-00343-2.
52. Sticht, C.; De La Torre, C.; Parveen, A.; Gretz, N. miRWalk: An online resource for prediction of microRNA binding sites. *PloS one* **2018**, *13*, e0206239, doi:10.1371/journal.pone.0206239.